

AD-A036 290

DEFENCE RESEARCH ESTABLISHMENT OTTAWA (ONTARIO)  
THE CYCLIC VOLTAMMETRY OF LEAD AND LEAD-ANTIMONY BATTERY GRID A--ETC(U)  
FEB 77 T G CHANG, M M WRIGHT, E M VALERIOTE

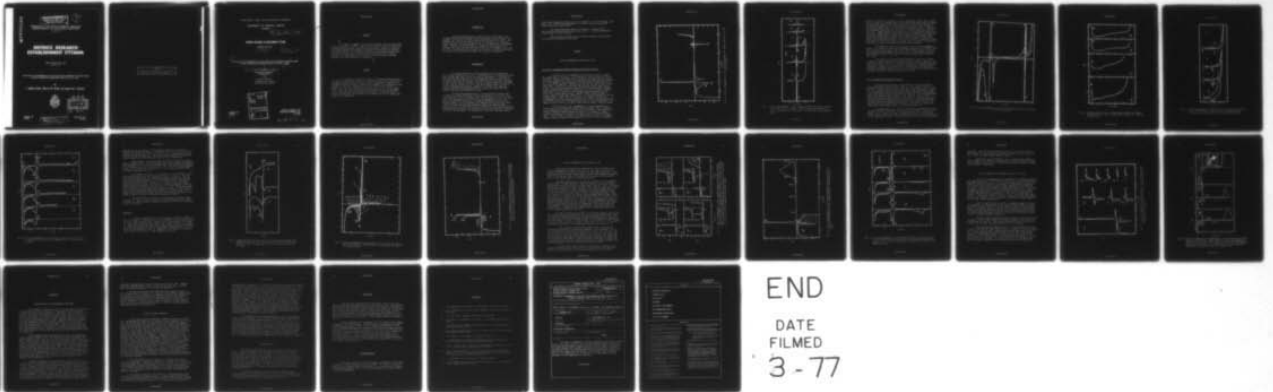
F/G 10/3

UNCLASSIFIED

DREO-R-753

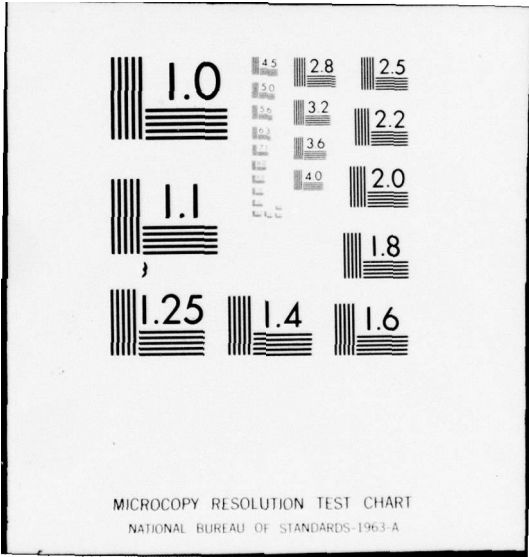
NL

1 of 1  
ADA036290



END

DATE  
FILMED  
3 - 77



MICROCOPY RESOLUTION TEST CHART  
NATIONAL BUREAU OF STANDARDS-1963-A

ADA 036290

**DISTRIBUTION STATEMENT A**  
Approved for public release:  
Distribution Unlimited

*(Handwritten initials and 'B.S.' in a circle)*

RESEARCH AND DEVELOPMENT BRANCH  
DEPARTMENT OF NATIONAL DEFENCE  
CANADA

# DEFENCE RESEARCH ESTABLISHMENT OTTAWA

DREO REPORT NO. 753  
DREO R 753

THE CYCLIC VOLTAMMETRY OF LEAD AND LEAD-ANTIMONY BATTERY GRID  
ALLOY IN AQUEOUS SULPHURIC ACID AT 25° TO -40°C

by

T. Godfrey Chang, Maurice M. Wright and Eugene M.L. Valeriote



**DDC**  
**RECEIVED**  
MAR 3 1977  
**RECEIVED**

*(Handwritten initials and 'C' in a circle)*

PROJECT NO.  
54-80-08

**DISTRIBUTION STATEMENT A**  
Approved for public release:  
Distribution Unlimited

FEBRUARY 1977  
OTTAWA

**CAUTION**

This information is furnished with the express understanding that proprietary and patent rights will be protected.

RESEARCH AND DEVELOPMENT BRANCH

DEPARTMENT OF NATIONAL DEFENCE  
CANADA

14 DREQ-R-753

DEFENCE RESEARCH ESTABLISHMENT OTTAWA

REPORT NO. 753 ✓

12 34 pgs

11 Feb 77

6

THE CYCLIC VOLTAMMETRY OF LEAD AND LEAD-ANTIMONY BATTERY GRID  
ALLOY IN AQUEOUS SULPHURIC ACID AT 25 TO -40°C

by

10

T. Godfrey/Chang and Maurice M./Wright

deg

Cominco Ltd., Sheridan Park,  
Mississauga, Ontario

and

Eugene M.L./Valeriot

Rechargeable Systems Section  
Electrical Power Sources Division

PROJECT NO.  
54-80-08

77-025

ACCESSION for	
NDS	White Section <input checked="" type="checkbox"/>
DDC	Buff Section <input type="checkbox"/>
UNANNOUNCED	<input type="checkbox"/>
JUSTIFICATION .....	
BY .....	
DISTRIBUTION/AVAILABILITY CODES	
Dist.	AVAIL. and/or SPECIAL
A	

RECEIVED JANUARY 1977  
PUBLISHED FEBRUARY 1977  
OTTAWA

404 576 LB

UNCLASSIFIED

ABSTRACT

↙  
The cyclic voltammetry of lead and antimonial lead has been studied in 1.25 S.G.  $H_2SO_4$ , at  $25^\circ C$  to  $-40^\circ C$ , at sweep rates of 0.42 to 42 mV/s, between hydrogen and oxygen evolution and over narrower regions of potential. The latter, coupled with systematic variation of the positive or negative reversal potential, has revealed peak shifting and hysteresis effects which give further insight into the nature of the reactions of the lead-acid battery. The significance of the results to the improvement of charge acceptance at low temperatures is discussed.

↑  
RÉSUMÉ

La coulométrie cyclique du plomb et de l'alliage plomb-antimoine a été étudiée à une densité d' $H_2SO_4$  de 1,25 entre  $25^\circ C$  et  $-40^\circ C$ , avec des taux de balayage variant de 0,42 à 42 mV/s, entre le dégagement d'hydrogène et d'oxygène et dans des zones de tension plus limitées. À ce dernier cas était imposée une variation systématique de potential d'inversion positif ou négatif qui a révélé un décalage de pointe de charge et une trainée magnétique. Ceci nous permet donc de mieux comprendre la nature des réactions qui se produisent dans un accumulateur plomb-acide. Le présent rapport traite de l'importance des résultats pour l'amélioration de la charge admissible à basse température.

(i)

NON-CLASSIFIÉ

### INTRODUCTION

Several investigators have reported on the linear sweep cyclic voltammetry of lead and antimonial lead in sulphuric acid solution at  $\sim 25^{\circ}\text{C}$  (Panesar, 1971; Carr et al, 1971; Sharpe, 1975; Brennan et al, 1974). Our purpose was to extend such studies to  $-40^{\circ}\text{C}$  in the context of the poorer charge acceptance of the lead-acid battery at low temperatures (Willihnganz, 1975). Valeriotte and Gallop (1975), in a study of the kinetics of the positive electrode, have reported some limited cyclic voltammetry at as low as  $-50^{\circ}\text{C}$ . The present work is further to the latter; it reveals more detail on the positive electrode and includes the region of the negative.

### EXPERIMENTAL

The test electrode was a disc measuring 1.9 cm in diameter by 0.1 cm thick, exposed area  $6.5\text{ cm}^2$ . An attached neck, 0.5 cm wide and coated with an epoxy resin mask, served as conductor and support. Electrodes of pure lead (99.997+ % Pb) were cut from continuous cast sheet and those of antimonial lead from rolled sheet. The composition of the latter (in weight %) was 3.5% Sb, 0.5% As, 0.18% Sn, 0.04% Cd, a typical commercial grid alloy. In each case the surface (as cast or as rolled) was prepared for electrolysis by degreasing with acetone, dipping for 1 minute in an ammonium acetate - acetic acid stripping solution to remove the oxide film, then rinsing with water and drying with acetone.

The test electrode was held in a vertical position between and 1 cm from two counter electrodes of pure lead (each  $6 \times 2 \times 0.1\text{ cm}$ ). The electrolyte was 1.25 S.G. sulphuric acid ( $425\text{ gm H}_2\text{SO}_4/1$ ), 65 ml. The glass cell (4 cm in diameter by 10 cm long) also accommodated a gas lift for gentle circulation (5 ml  $\text{N}_2/\text{min.}$ ), a sheathed thermocouple, and reference electrode probe. The cell assembly was suspended from a glass tube, 24 cm long by 18 mm OD, through which passed the electrical leads and other services, and on top of which was a small chamber for the reference electrode. Connection of the latter to the probe was by way of the same acid electrolyte in 35 cm of 4mm OD tubing. By this means the reference electrode could be

held at room temperature while the cell was immersed in a cold air bath. The latter was a thermostated arrangement in a 8-litre stainless steel Dewar flask using dry ice as coolant.

The linear potential sweep was provided by a Wenking TR-61 potentiostat with Wenking MP-64 motor potentiometer. Current and potential were recorded on an x-y recorder.

The reference electrode was the saturated calomel electrode (SCE). All potentials are given on this scale.

## RESULTS

### CYCLIC VOLTAMMETRY ON PURE LEAD AT 25°C

#### THE CYCLIC VOLTAMMOGRAM BETWEEN HYDROGEN AND OXYGEN EVOLUTION

A typical cyclic voltammogram for pure lead is shown in Figure 1, at a sweep ratio of 4.17 mV/s. It is similar in several respects to those reported by Panesar (1971) and Carr et al (1971), at sweep rates of 0.5 and 58.3 mV/s, respectively. Thus, in the positive sweep from hydrogen evolution ( $\sim -1.3V$ ) through to oxygen evolution ( $\sim 2.0V$ ), the only anodic peak to be seen is at  $-0.5V$  (peak IX). Panesar (1971) reports the same result, as does Feder (1971). Carr et al (1971) find this peak plus a very small one at  $-0.35V$ . Reversing direction and returning on the negative sweep a complex mixture of anodic and cathodic activity occurs at  $\sim 1.5V$  and major cathodic peaks appear at  $-0.4$  and  $-0.6V$ , each having a negative shoulder and the latter also a large negative wing. Panesar's (1971) negative sweep is similar though he finds less complexity at  $\sim 1.5V$  and no shoulders on the two cathodic peaks. Sharpe (1975), in a study that examined the negative voltammogram of the pre-anodized surface (up to 1 hour at various potentials) reports activity in the 1.5-V region very similar to that observed here. His sweep rate was 0.5 mV/s. Carr et al (1971) did not report a negative sweep.

The form of the cyclic voltammogram is largely independent of sweep rate, as also reported by Panesar (1971) and Feder (1971). However, it does depend on the number of cycles and on the amount of anodization preceding the negative sweep, whether the latter is by holding at a given current or potential, or by going to a higher positive reversal potential (prp). Thus, as shown in Figure 2, the mixed activity in the 1.5-V region changes in form as anodization increases from a prp of 1.9V to an anodizing

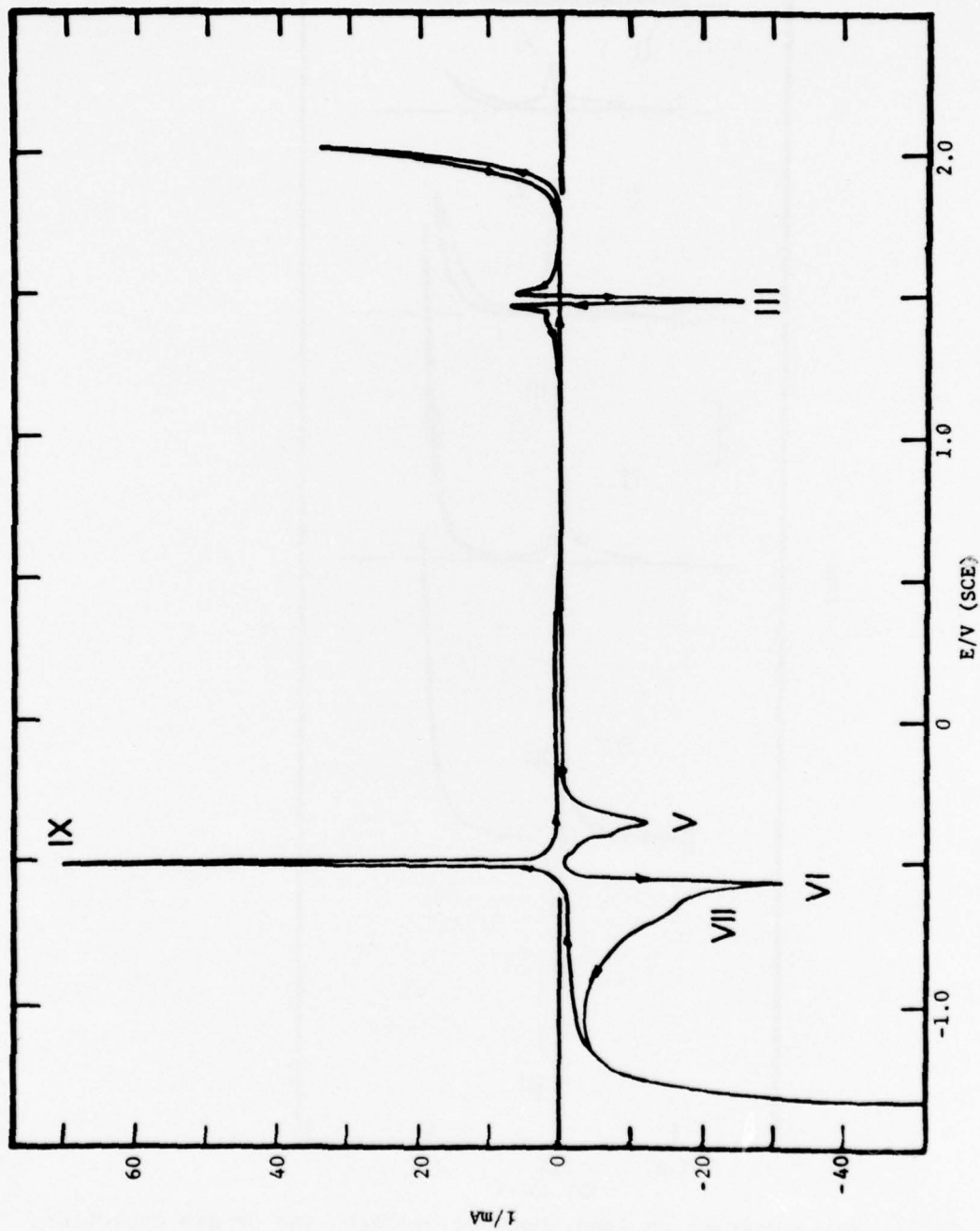


Fig. 1. Cyclic voltammogram on lead, between hydrogen and oxygen evolution, at 25°C and 4.17 mV/s.

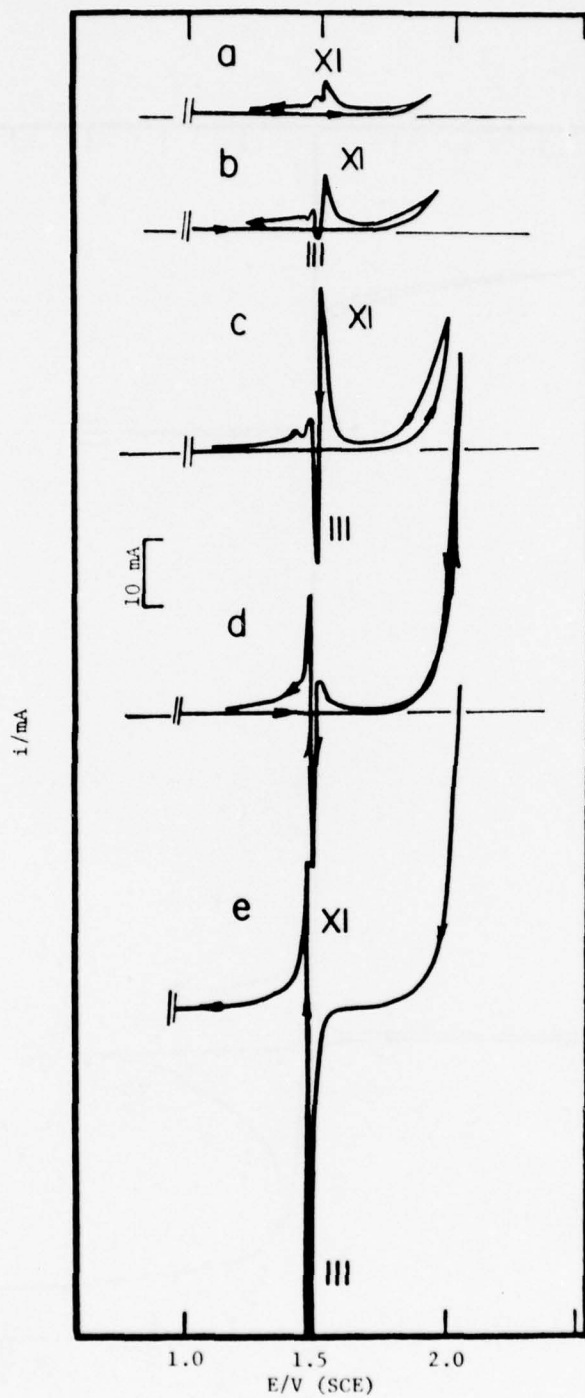


Fig. 2. Cyclic voltammograms on lead, between hydrogen and oxygen evolution, at 25°C and 4.17 mV/s, showing effect of increasing anodization. In (e) anodization was at 8 mA/cm<sup>2</sup> for 1 min prior to the negative sweep.

current of  $8 \text{ mA/cm}^2$  for 1 minute ( $\sim 2.1\text{V}$ ): from anodic activity with a small valley at  $1.5\text{V}$ , to a cathodic peak at  $1.5\text{V}$  with anodic peaks before and after, to the cathodic peak at  $1.5\text{V}$  with anodic activity only on the negative side. The latter configuration is the one reported by Panesar (1971). Further, the cathodic peak at  $-0.4\text{V}$ , as indicated by the negative shoulder, represents two overlapping activities, one at  $-0.37$  to  $-0.40\text{V}$ , b, and one at  $-0.42$  to  $-0.45\text{V}$ , a. Commencing with a new surface only b is observed during the first few cycles. With further cycling a appears and as the amount of anodization increases a becomes large relative to b. Eventually this composite peak, peak V, may become larger than the one at  $-0.6\text{V}$ . Likewise, in the early cycles on a new surface the peak at  $-0.6\text{V}$  can be seen as a composite of three activities: at  $-0.6$ ,  $-0.85$ , and  $-1.1\text{V}$  (peaks VI, VII, and VIII, respectively). With further cycling VIII disappears and VII shifts positive.

Two additional features can be seen in the cyclic voltammogram of Figure 3, at  $1.38 \text{ mV/s}$ . Shown on the expanded current scale is a small anodic peak at  $-0.5\text{V}$  in the negative sweep, and a small cathodic peak at  $-0.6\text{V}$  in the following positive sweep. The latter is also seen at higher rates when the electrode is new and the negative reversal potential (nrp) is greater than  $-0.8\text{V}$ .

The region of the positive sweep between  $-0.5$  and  $1.5\text{V}$  is shown in Figure 4, at four sweep rates between  $0.42$  and  $41.7 \text{ mV/s}$ . There is a low level of activity in the form of several plateaus of increasing height rather than peaks. However, one of us (E.M.L.V.) in addition to finding a plateau structure of at least two sections (at  $15^\circ$  and  $0.5 \text{ mV/s}$ ), has also often observed clear anodic peaks at  $0.1\text{V}$ , for both stationary and rapidly rotating horizontal electrodes. Perhaps geometry is a factor.

#### CYCLIC SWEEPING WITHIN SELECTED REGIONS

When the negative sweep is reversed above  $\sim 0\text{V}$  two additional anodic peaks appear in the positive sweep: at  $\sim 1.5\text{V}$  (peak I) and at  $\sim 1.8$  (peak II). This is shown in Figure 5, for nrp of  $0.95\text{V}$  and cycles 1 through 10. With repeated cycling the two peaks become larger and undergo a small shift in potential, peak I becoming more positive and peak II more negative. At the same time their definition improves, although a large overlap between peak II and oxygen evolution remains. With reduction in nrp to  $0.1\text{V}$  (Figure 6) both peaks shift positive, I more than II. The negative sweep in this region is also changed: beyond the second cycle (Figure 5) the anodic activity vanishes and cathodic peaks occur at  $1.45\text{V}$  (peak III) and  $\sim 1.2\text{V}$  (peak IV), the latter very small. Systematic variation of prp shows that anodic peak II and cathodic peak III are related (Figure 7).

Cathodic peak V, at  $\sim -0.4\text{V}$ , is affected by the potential at which the positive sweep is reversed. Thus, for a prp less than  $\sim 1.0$  peak V is absent. Above  $\sim 1.0\text{V}$  it increases in magnitude and shifts negative with increase in prp (Figure 8). Panesar (1971) also reports a critical potential for the appearance of peak V, this peak appearing only when the electrode was

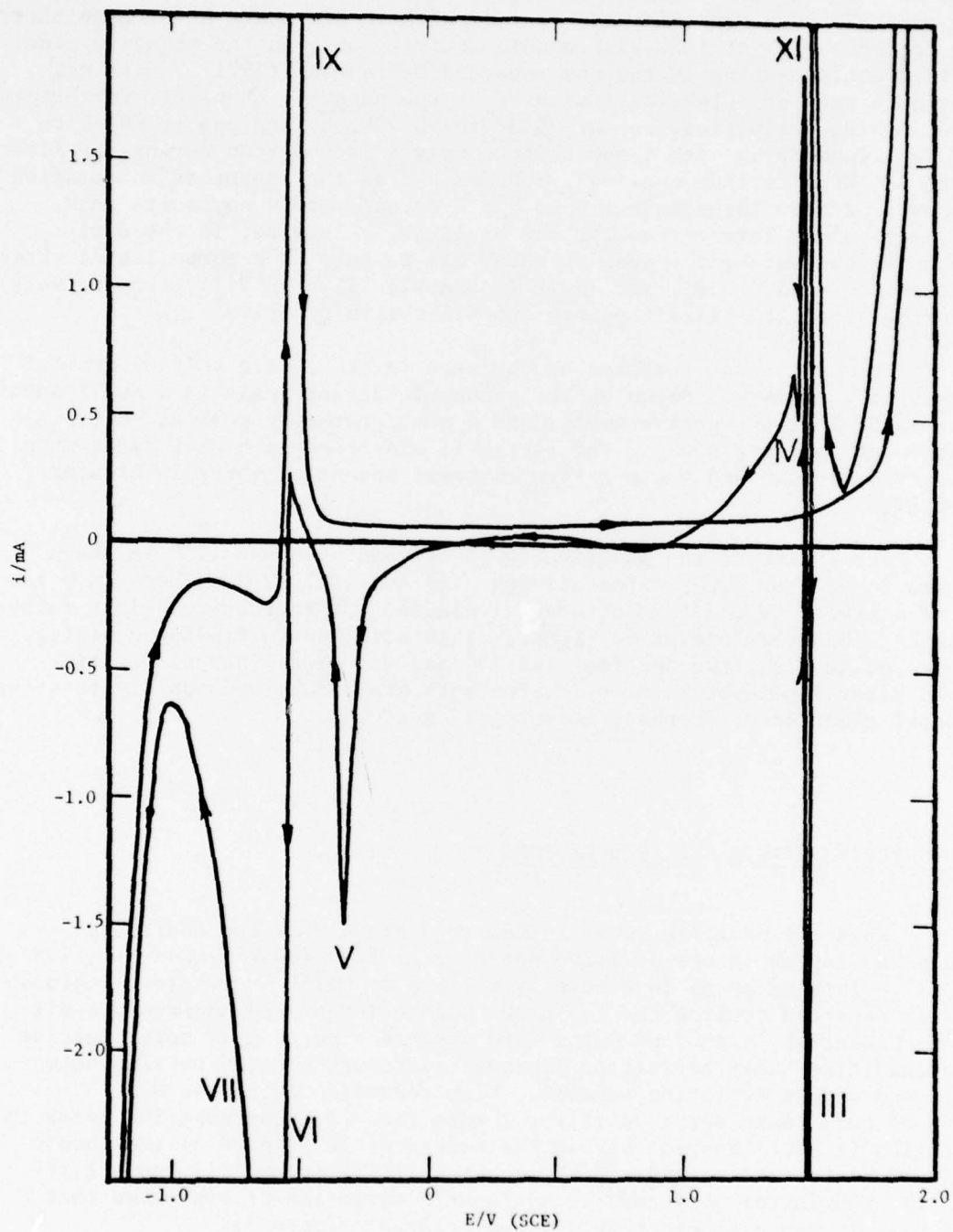


Fig. 3. Cyclic voltammogram on lead, between hydrogen and oxygen evolution, at 25°C and 1.38 mV/s.

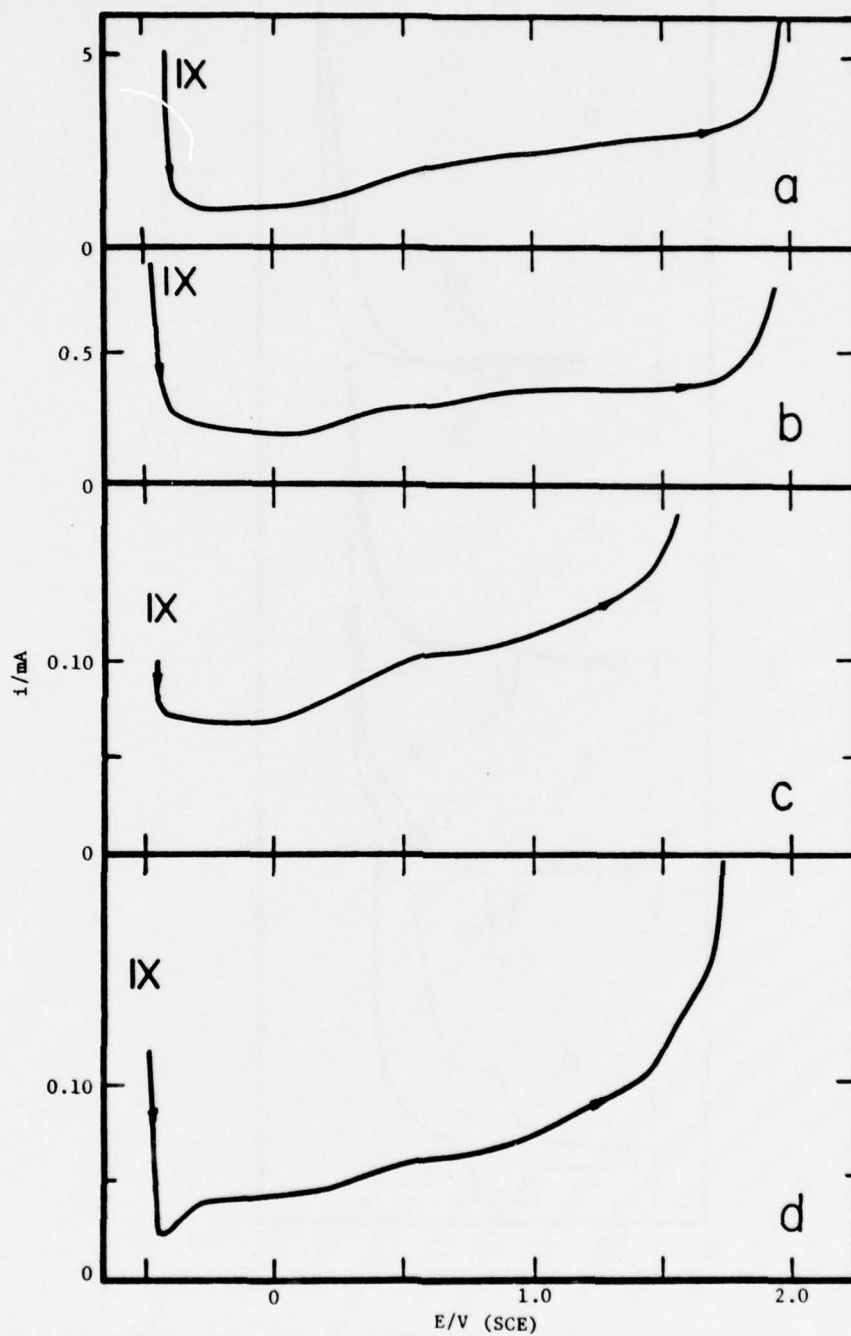


Fig. 4. Positive sweeps on lead, cycling between hydrogen and oxygen evolution, at 25°C: (a) 41.7 mV/s, (b) 13.9 mV/s, (c) 1.39 mV/s, (d) 0.42 mV/s.

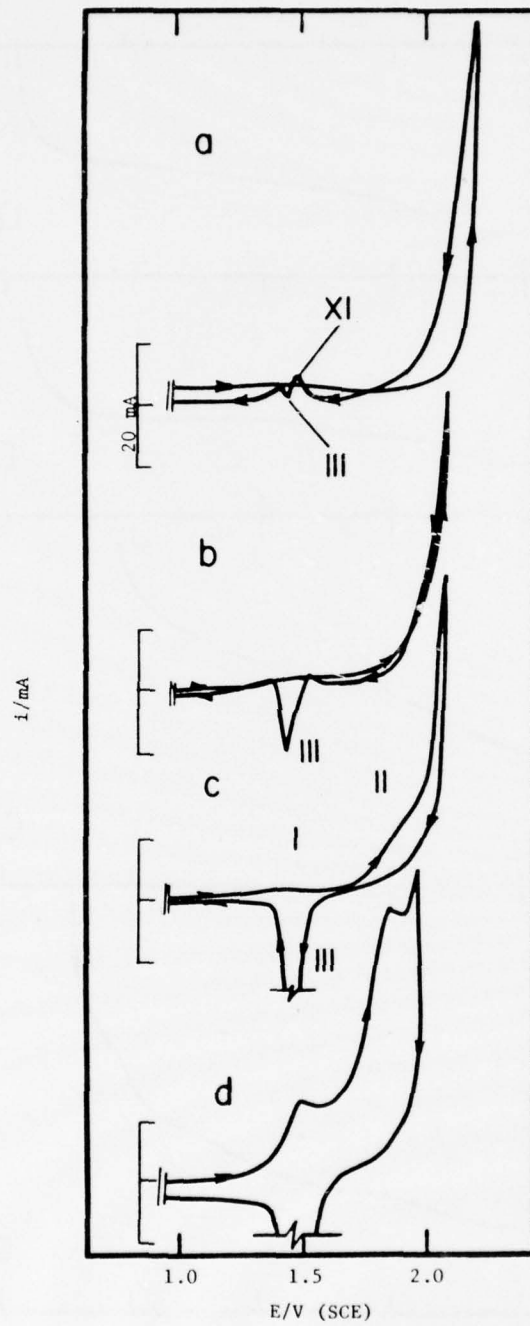


Fig. 5. Cyclic voltammograms on lead, between 0.95V and oxygen evolution, at 25°C and 41.7 mV/s, showing effect of repeated cycling: (a) 1st cycle, (b) 2nd cycle, (c) 4th cycle, (d) 10th cycle.

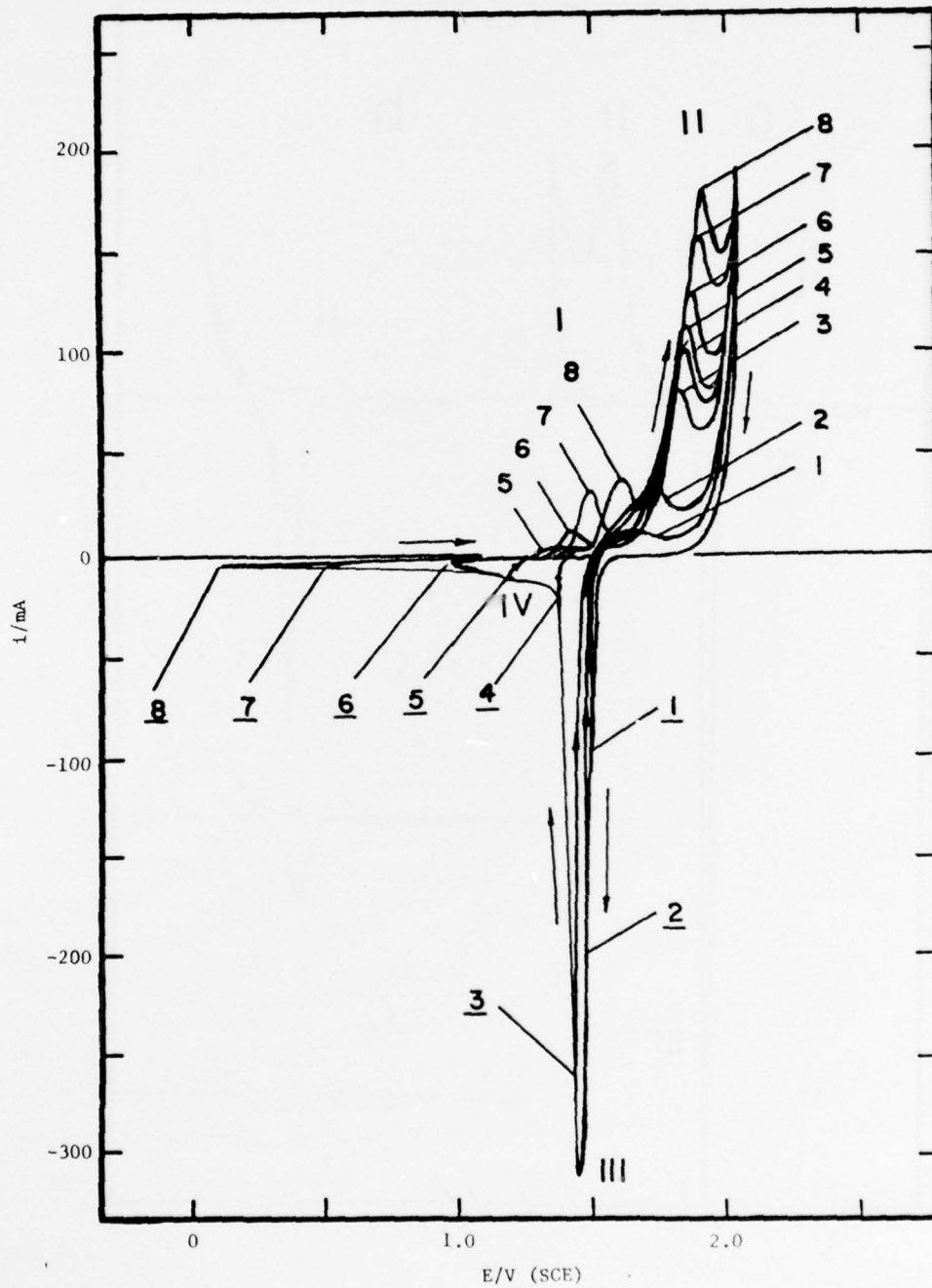


Fig. 6. Cyclic voltammograms on lead, between 1.5 to 0.1V and oxygen evolution (2.05V), at 25°C and 41.7 mV/s, showing effect of decreasing nrp on peaks I and II.

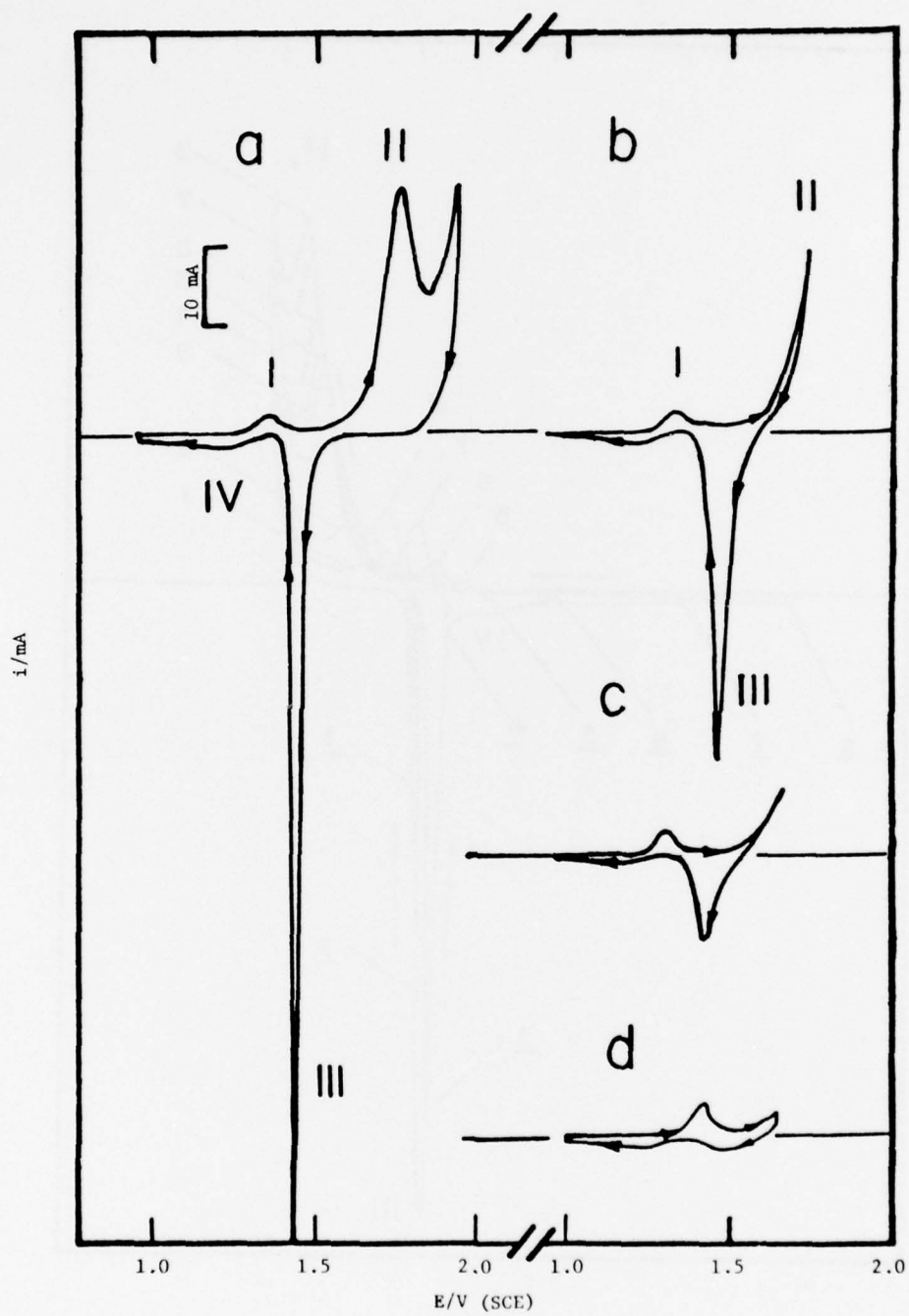


Fig. 7. Cyclic voltammograms on lead, between 1.0V and 1.95 to 1.65V, at 25°C and 4.17 mV/s, showing effect of decreasing prp on peak III.

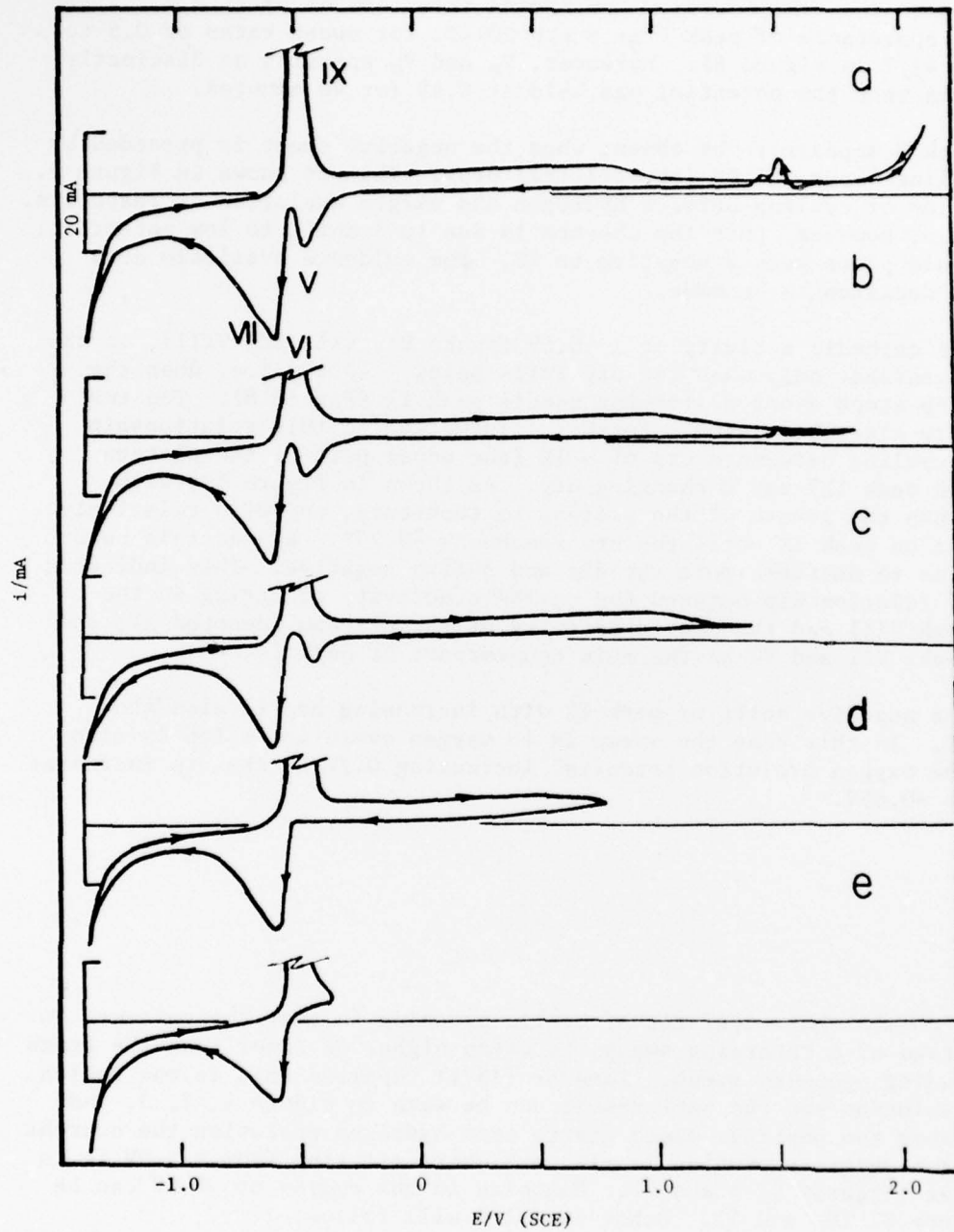


Fig. 8. Cyclic voltammograms on lead, between hydrogen evolution and 2.1 to -0.4V, at 25°C and 41.7 mV/s, showing effect of decreasing prp on peak V.

anodized at 0.2V for 16 hours. The difference between 1.0 and 0.2V is evidently due to the time factor. Confirming this, one of us (E.M.L.V.) has observed the appearance of peak V at a prp  $\geq 0.4V$ , for sweep rates of 0.5 to 2.0 mV/s (vs 41.7 in Figure 8). Moreover,  $V_a$  and  $V_b$  appeared as distinctly separate peaks when the potential was held at 0.4V for 40 minutes.

Peak V appears to be absent when the negative sweep is preceded by repeated cycling above  $\sim 1.0V$  (the critical prp). This is shown in Figure 9. With resumption of cycling between hydrogen and oxygen evolution it reappears. It is possible, however, that the absence is due to a shift to low potential, though it would place peak V negative to IX. The evidence available does not permit a decision to be made.

The cathodic activity at  $\sim -0.6V$  (peaks VI, VII, and VIII), on the other hand, vanishes only when the prp falls below  $\sim -0.5V$ , i.e. when the positive sweep stops short of forming anodic peak IX (Figure 8). The two activities are clearly related. Further information on this relationship is given by cycling between a prp of  $\sim 1V$  (the upper part of the plateau region beyond peak IX) and a changing nrp. As shown in Figure 10, with increase in nrp the length of the plateau is shortened, and with relatively little effect on peak IX until the nrp reaches  $\sim -0.75V$ . Beyond this point peak IX begins to decrease more rapidly and shifts negative. This indicates some type of relationship between the cathodic activity occurring in the region of peak VIII and the anodic activity of the plateau (denoted X), and points to peaks VII and VI as the main counterpart of peak IX.

The negative shift of peak IX with increasing nrp is also shown in Figure 11. In this case the sweep is to oxygen evolution which is also affected, the oxygen evolution potential increasing 0.2V as the nrp increases from -0.9 to -0.65V.

#### HYSTERESIS

A common characteristic of cyclic sweeping is that the current, in the early stage of a returning sweep, is often higher or lower than the trace of the preceding opposite sweep. Panesar (1971) reported this in the region of oxygen evolution and the same result can be seen in Figure 1, 2, 3, and 11. Thus, when the positive sweep starts from hydrogen evolution the current returning from oxygen evolution is always higher; starting from  $> \sim 0V$  it is usually lower (Figures 5, 6 and 7). Examples in the region of -0.5V can be seen in Figure 8, 10, and 11. Other examples will follow.

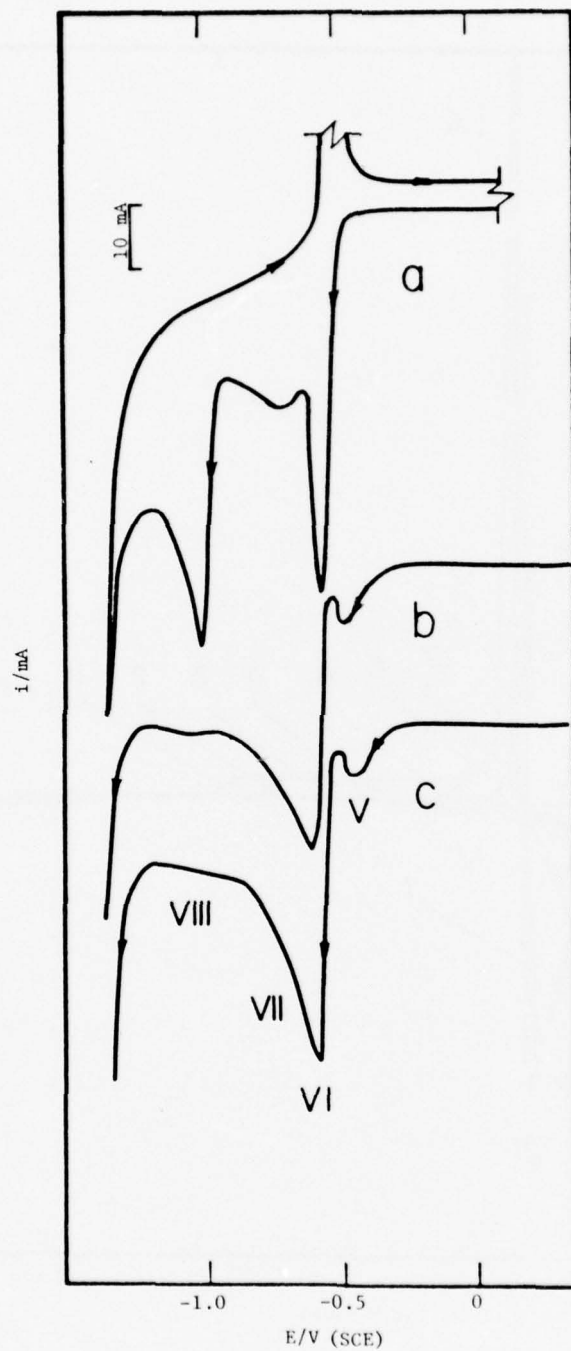


Fig. 9. Consecutive negative sweeps on lead, cycling between hydrogen and oxygen evolution (-1.4 to 2.1V), the electrode having been cycled between 1.0 and 2.1V immediately prior to sweep (a), at 25°C and 41.7 mV/s.

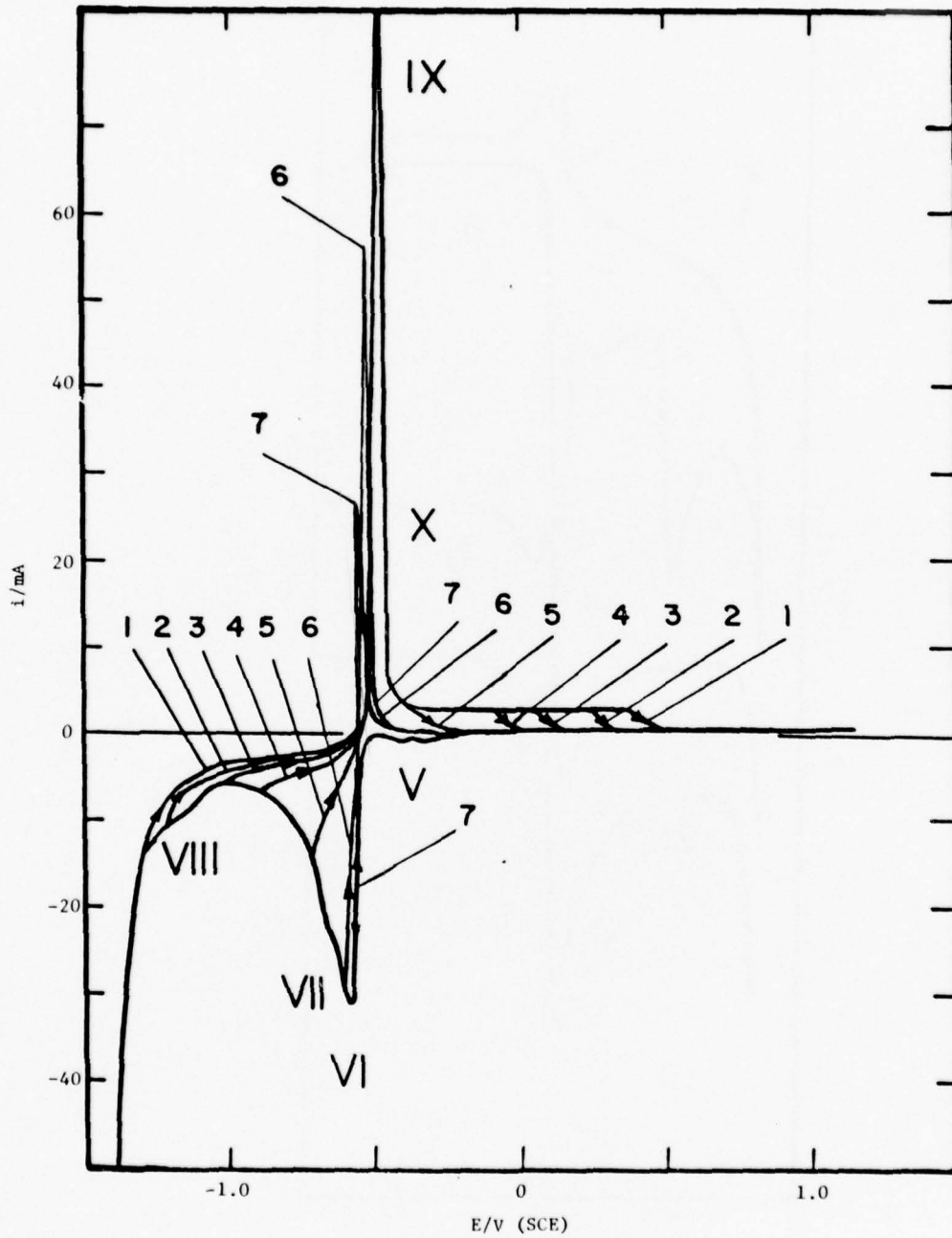


Fig. 10. Cyclic voltammograms on lead, between -1.4 to -0.6V and 1.15V, at 25°C and 13.9 mV/s, showing effect of increasing nrp on peak IX and plateau region.

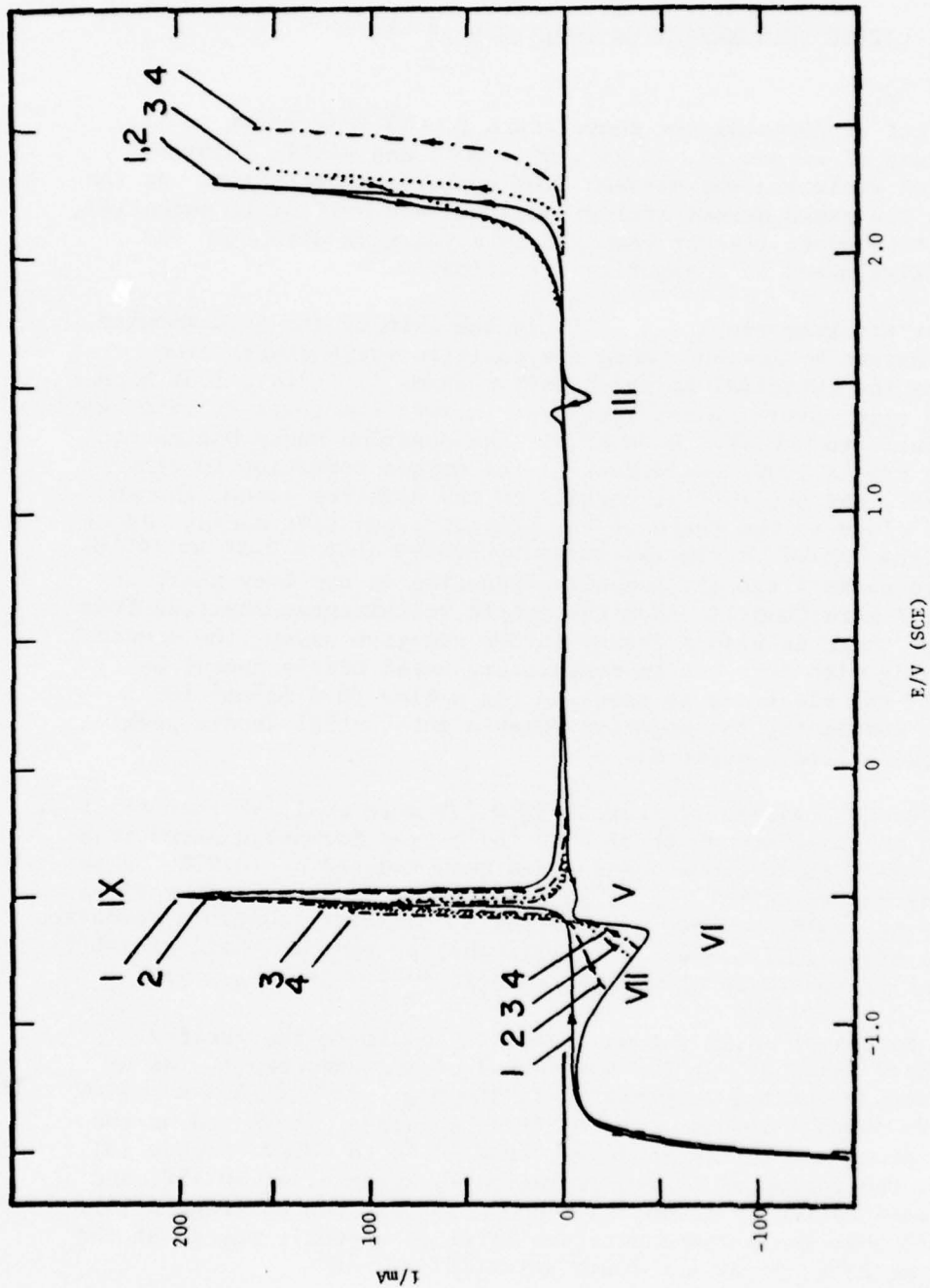


Fig. 11. Cyclic voltammograms on lead between -1.5 to -0.65V and oxygen evolution, at 25°C and 41.7 mV/s, showing effect of increasing nrp on peak IX and oxygen evolution potential.

CYCLIC VOLTAMMETRY ON PURE LEAD AT  $-40^{\circ}\text{C}$ 

The effect of lowering the temperature to  $-40^{\circ}\text{C}$  is shown in the cyclic voltammograms of Figure 12, at  $25^{\circ}$ ,  $0^{\circ}$ ,  $-20^{\circ}$ , and  $-40^{\circ}\text{C}$ , between hydrogen and oxygen evolution and between  $1.0\text{V}$  and oxygen evolution. As the temperature falls the peaks become smaller and they are shifted in potential, those of the positive sweep (except peak IX) in a positive direction and those of the negative sweep in a negative direction.

The most striking result at  $-40^{\circ}\text{C}$  is the form of the voltammogram in the region of oxygen evolution. When the positive sweep starts from hydrogen evolution the potential at which oxygen forms is  $\sim 3.4\text{V}$ ,  $1.3\text{V}$  higher than at  $25^{\circ}\text{C}$ , and upon reversing the sweep the current continues to rise until the potential returns to  $\sim 2.7\text{V}$ . However, if the positive sweep begins at  $1.0\text{V}$  (i.e. if the nrp is  $1.0\text{V}$ ) the potential for oxygen formation is only  $\sim 2.3\text{V}$ ,  $0.2\text{V}$  higher, and the initial current in the negative sweep, though still greater, is close to the trace of the preceding positive sweep. As at  $25^{\circ}\text{C}$ , it is only the latter of the two positive sweeps (nrp  $\geq 0.5\text{V}$  at  $-40^{\circ}\text{C}$ ) that gives rise to peaks I and II, and with reduction in nrp they shift to higher potential, I more than II. For the cyclic voltammogram starting from hydrogen evolution there is also a change in the negative sweep, the anodic activity diminishing with decrease in temperature until nearly absent at  $-40^{\circ}\text{C}$ . However, if the electrode is anodized for a time ( $0.8\text{ mA/cm}^2$  for 5 minutes) prior to commencing the negative sweep a substantial anodic peak (XI) is found [Figure 12(d), curve B].

At  $-40^{\circ}\text{C}$  the position of peak II is  $0.27\text{V}$  more positive than at  $25^{\circ}\text{C}$ . This coupled with the positive shift of  $0.2\text{V}$  for oxygen formation means that the separation between these two processes has been reduced by  $\sim 0.07\text{V}$ . This can be seen in the poorer definition of peak II in Figure 12(d). Peak II is also much smaller at  $-40^{\circ}\text{C}$ ,  $\sim 1/500$  its size at  $25^{\circ}\text{C}$ . There is also a reduction in the size ratio of peak II to peak I, from  $\sim 10/1$  at  $25^{\circ}\text{C}$  to  $\sim 1/1$  at  $-40^{\circ}\text{C}$ . The ratio of peaks III to IV is similarly reduced, from  $\sim 20/1$  to  $\sim 2/1$ .

In the region of  $-0.5\text{V}$  the most notable result is the greater importance of peak V and the improved resolution of its components. As at  $25^{\circ}\text{C}$ , the appearance of peak V is governed by the prp. At  $< 0.4\text{V}$  (vs  $\sim 1.0\text{V}$  at  $25^{\circ}\text{C}$ ) peak V is absent. Beyond  $0.4\text{V}$  the first to appear is  $V_b$  and as the nrp increases it grows and shifts negative, from  $-0.45$  to  $-0.6\text{V}$  (Figure 13). As the prp enters the region of oxygen evolution  $V_a$  appears, at  $-0.45\text{V}$ , and with increasing anodization it grows and becomes larger than  $V_b$  (Figure 14). It should be noted that the  $b$  component (the first to appear), though at the higher potential at  $25^{\circ}\text{C}$ , is at the lower potential at  $-40^{\circ}\text{C}$ .

The other peaks in this region are affected as follows by the reduction in temperature to  $-40^{\circ}\text{C}$ . Peak VIII becomes smaller and almost disappears below  $-20^{\circ}\text{C}$ . Peaks VI and VII become smaller, the ratio VII/VI

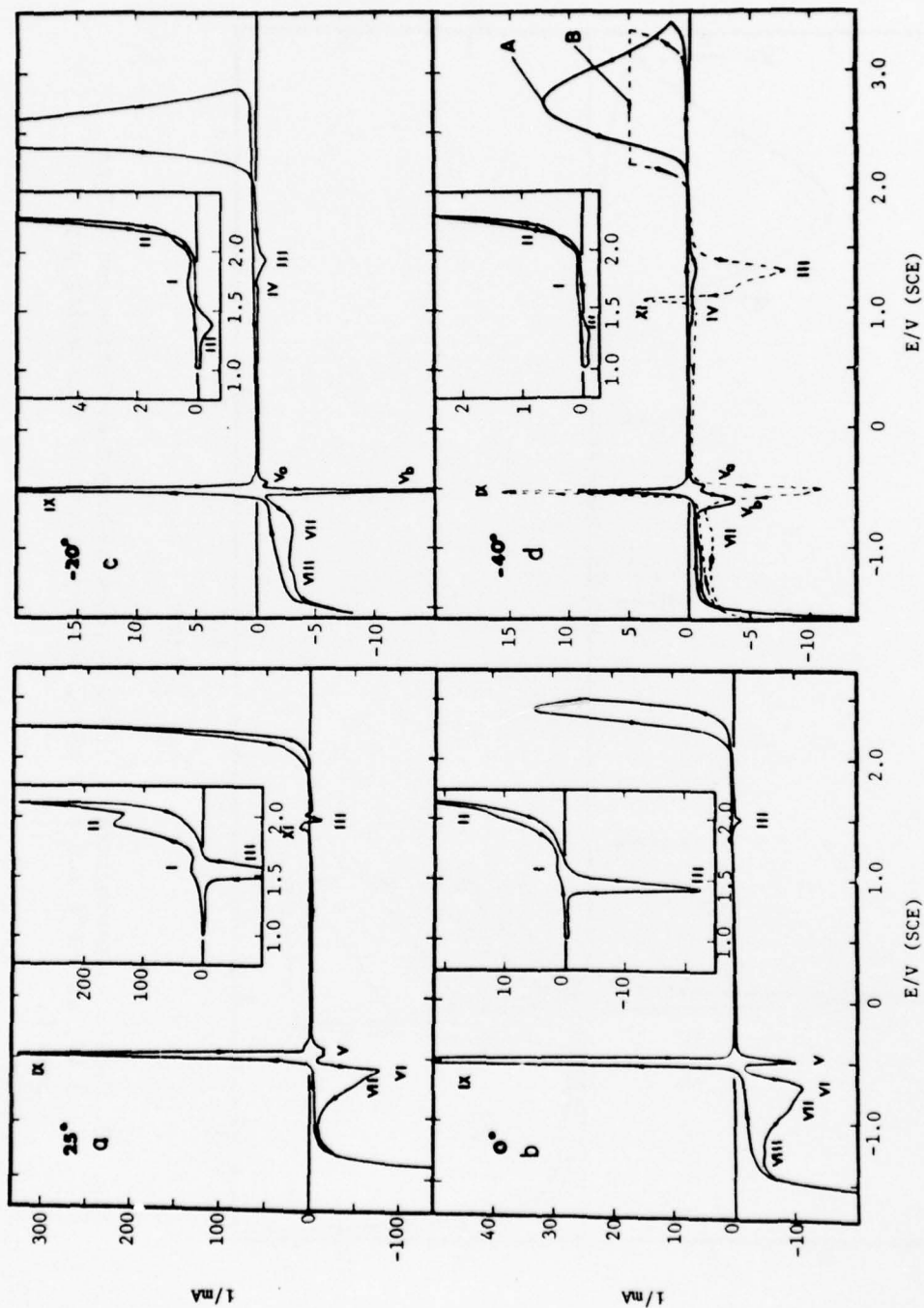


Fig. 12. Cyclic voltammograms on lead, between hydrogen and oxygen evolution and, inset, between 1.0V and oxygen evolution, at 41.7 mV/s, showing effect of decreasing temperature: (a) 25°, (b) 0°, (c) -20°, (d) -40°C. In B of (d) the electrode was anodized at 0.8 mA/cm<sup>2</sup> for 5 min (from 3.3 to 2.2V) prior to commencing the negative sweep.

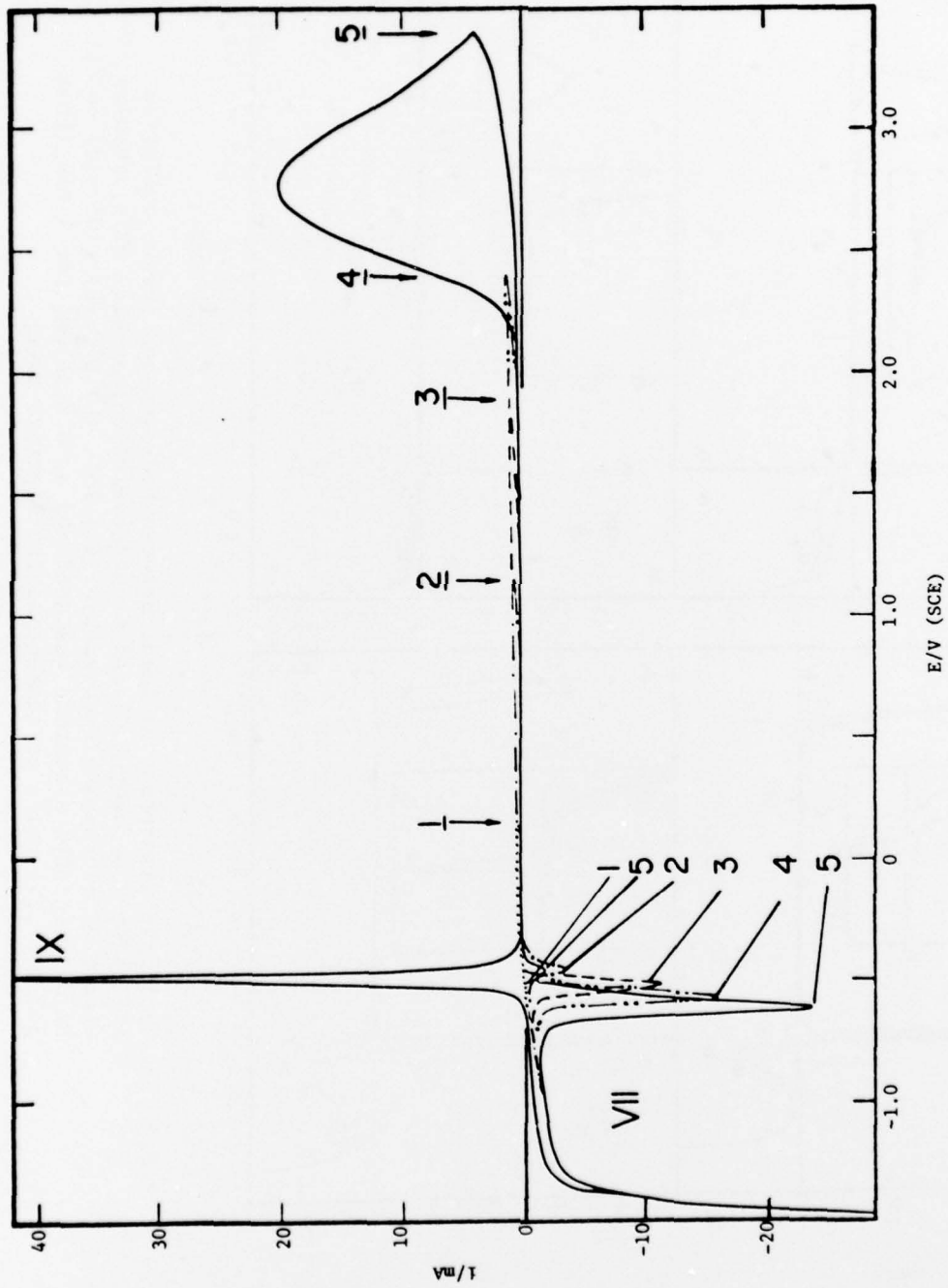


Fig. 13. Cyclic voltammograms on lead, between hydrogen evolution and 0.2 to 3.4V, at  $-40^{\circ}\text{C}$  and 41.7 mV/s, showing effect of increasing prp on peak V.

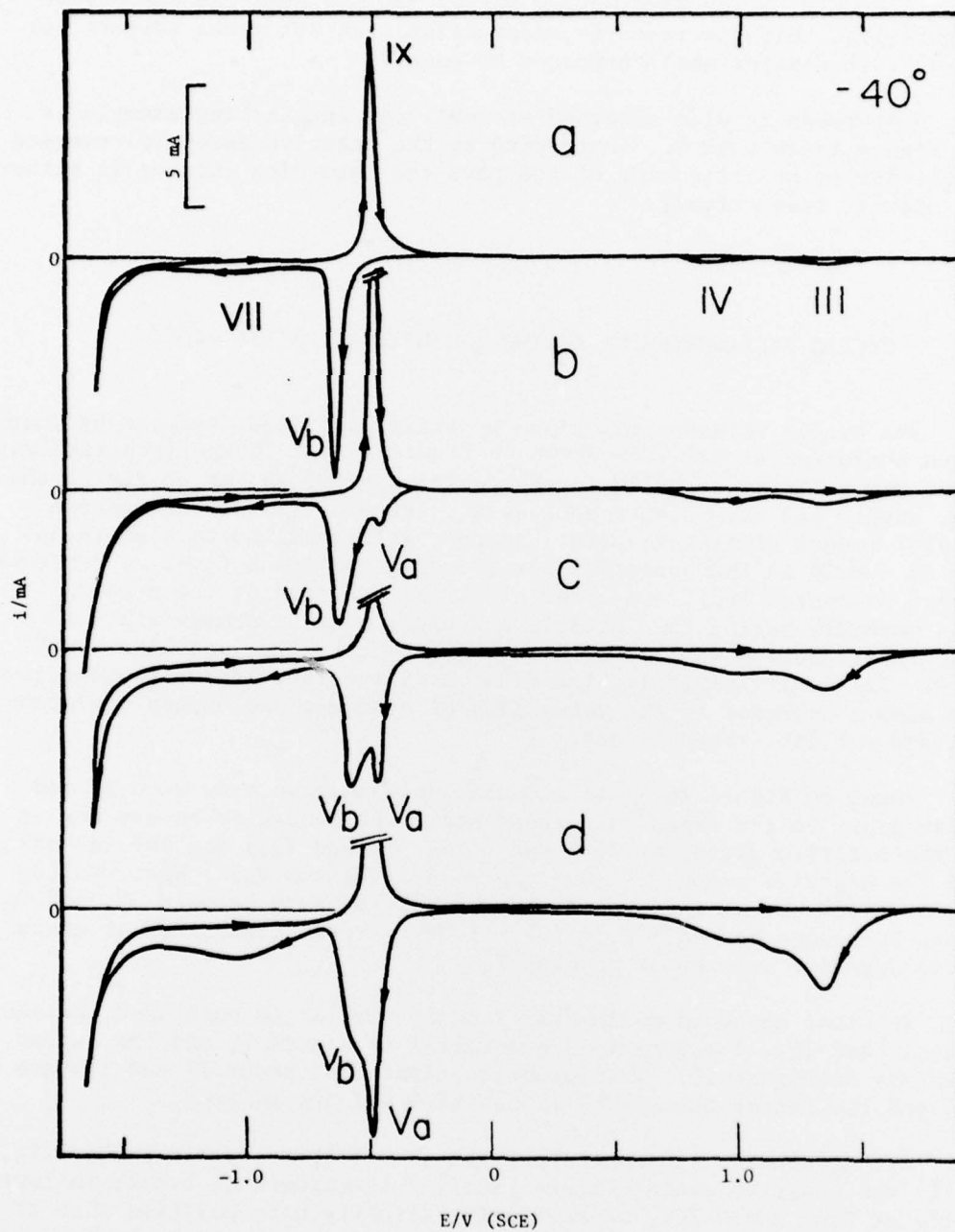


Fig. 14. Cyclic voltammograms on lead, between hydrogen and oxygen evolution at  $-40^{\circ}\text{C}$  and  $41.7 \text{ mV/s}$ , showing effect of increasing anodization on peak V: (a) to  $3.3 \text{ V}$ , (b) to  $3.5 \text{ V}$ , (c)  $3.1 \text{ mA/cm}^2$  for  $1.5 \text{ min}$ , (c)  $3.1 \text{ mA/cm}^2$  for  $3 \text{ min}$ .

increasing. By  $-10^{\circ}\text{C}$  they have merged and by  $-30^{\circ}\text{C}$  a peak can scarcely be seen (Figure 12). With increase in anodization peak VII grows (Figure 14) but, at  $-40^{\circ}$ , it remains small compared to peak V.

Hysteresis is also observed at  $-40^{\circ}$ . An interesting example is shown in Figure 15 on peak  $V_b$ . According as the negative sweep is reversed on the negative or positive side of the peak the returning current is either lower or higher, respectively.

#### CYCLIC VOLTAMMETRY ON ANTIMONIAL LEAD AT $25^{\circ}$ TO $-40^{\circ}\text{C}$

The cyclic voltammogram given by antimonial lead, between hydrogen and oxygen evolution at  $25^{\circ}\text{C}$ , is shown in Figure 16(a). Comparison with pure lead shows new activity at 0.12V in the positive sweep and at  $-0.22\text{V}$  in the negative, anodic and cathodic, respectively. Panesar (1971) and Brennan et al (1974) report similar results. Another difference to be seen is an increase of  $\sim 0.4\text{V}$  in the potential for hydrogen evolution (i.e., a decrease in hydrogen overpotential). On a new electrode the size of these peaks decreases markedly during the initial  $\sim 5$  cycles, until a steady state is reached. The reduction is  $\sim 80\%$  at 0.12V,  $\sim 50\%$  at  $-0.22\text{V}$ , and also  $\sim 50\%$  at peak V. They shift slightly, the first positive, the latter two negative. There is also a decrease in the potentials of hydrogen and oxygen evolution of  $\sim 0.1$  and  $\sim 0.15\text{V}$ , respectively.

Inset in Figure 16(a) is a cyclic voltammogram between 0.5V and a decreasing rrp. On the expanded current scale two anodic peaks can now be seen in the positive sweep, at 0.05 and 0.16V ( $I_S$  and  $II_S$ ) and two cathodic peaks in the negative sweep, at  $-0.2$  and  $-0.4\text{V}$  ( $IV_S$  and  $V_S$ ). When cycling is between  $-0.55\text{V}$  and an increasing prp, peak  $V_b$  appears between  $IV_S$  and  $V_S$  as the prp increases beyond  $\sim 0.5\text{V}$  (vs  $\sim 1.0\text{V}$  for pure lead), and it grows and shifts negative eventually masking  $V_S$ .

In other respects antimonial lead is similar to pure lead, as shown in Figure 17 and 18. The former is a parallel to Figure 7, and the latter complementary to Figure 10. The former confirms that peaks II and III are related, and the latter that peaks IX and VI + VII are related.

With reduction in temperature to  $-40^{\circ}\text{C}$  a third anodic peak,  $III_S$ , is seen in the positive sweep [Figure 16(c)]. It appears at 0.35V, following  $I_S$  and  $II_S$  at 0.07 and 0.20V, respectively, slightly more positive than at  $25^{\circ}$ . In the negative sweep  $IV_S$  and  $V_S$  appear at  $-0.5$  and  $-0.8\text{V}$ , having undergone a large negative shift. The size of these peaks is about 1/10 their size at  $25^{\circ}$ . The potential for hydrogen evolution remains  $\sim 0.4\text{V}$  more positive than for pure lead. As a result, peak VIII is fully masked and peak VII becomes a shoulder on the hydrogen evolution curve (Figure 16).

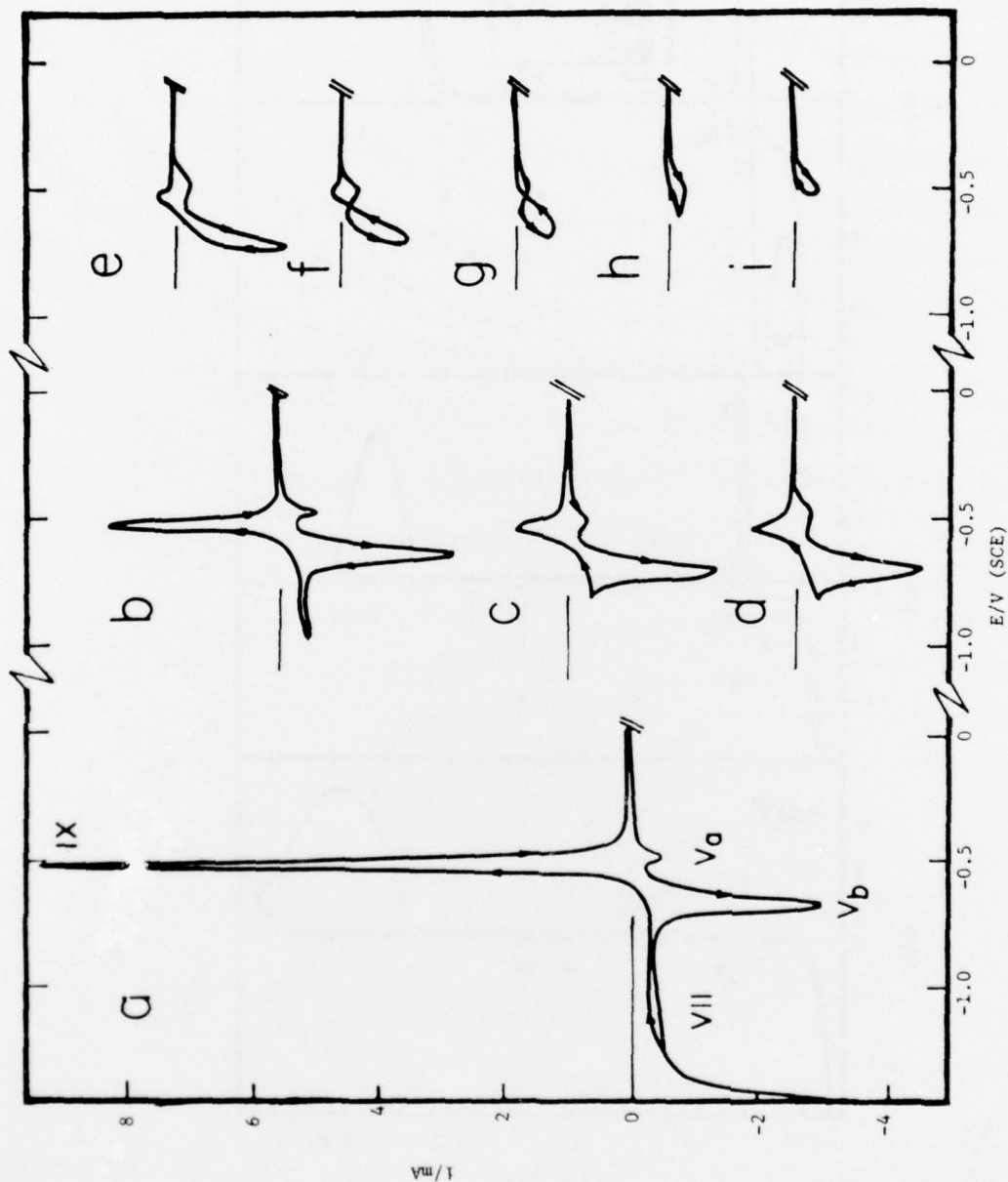


Fig. 15. Cyclic voltammograms on lead, between -1.5 to -0.5V and oxygen evolution (3.4V) at  $-40^{\circ}\text{C}$  and 41.7 mV/s, showing effect of increasing up on peak V.

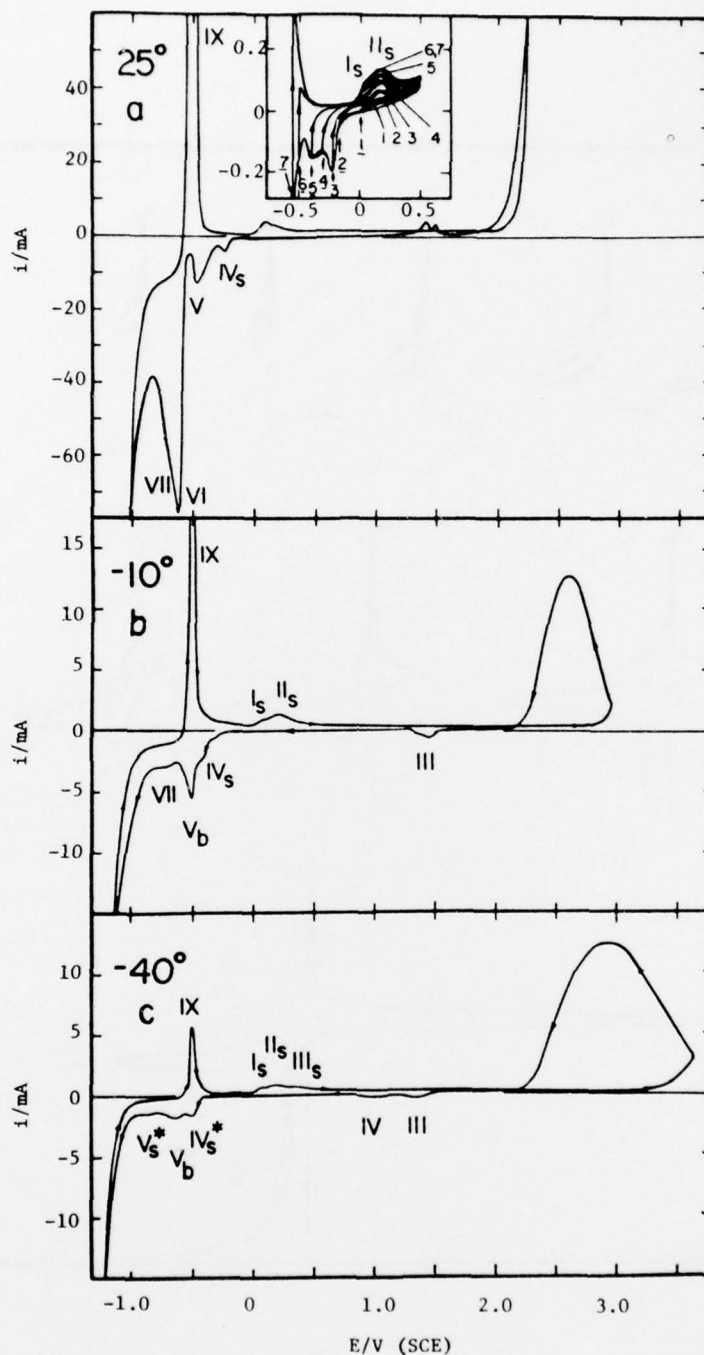


Fig. 16. Cyclic voltammograms on antimonial lead, between hydrogen and oxygen evolution, at 41.7 mV/s, showing effect of decreasing temperature: (a) 25°C, (b) -10°C, (c) -40°C. Inset in (a) are cyclic voltammograms between 0.0 to -0.55V and 0.5V, showing effect of decreasing nrp. \*Peak  $V_a$  may contribute to  $IV_s$ ; VII is masked by  $V_s$ .

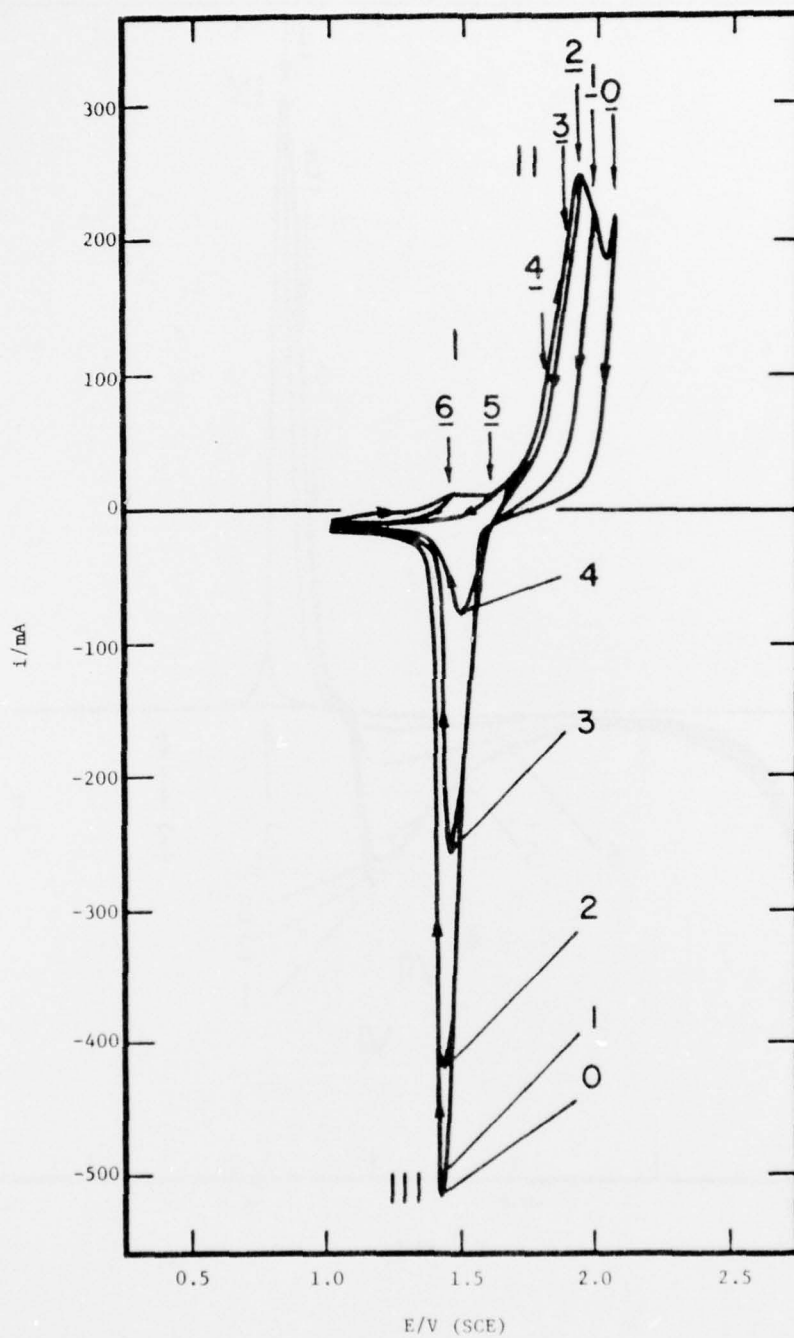


Fig. 17. Cyclic voltammograms on antimonial lead, between 1.0V and 2.1 to 1.4V, at 25°C and 41.7 mV/s, showing effect of decreasing prp on peak III.

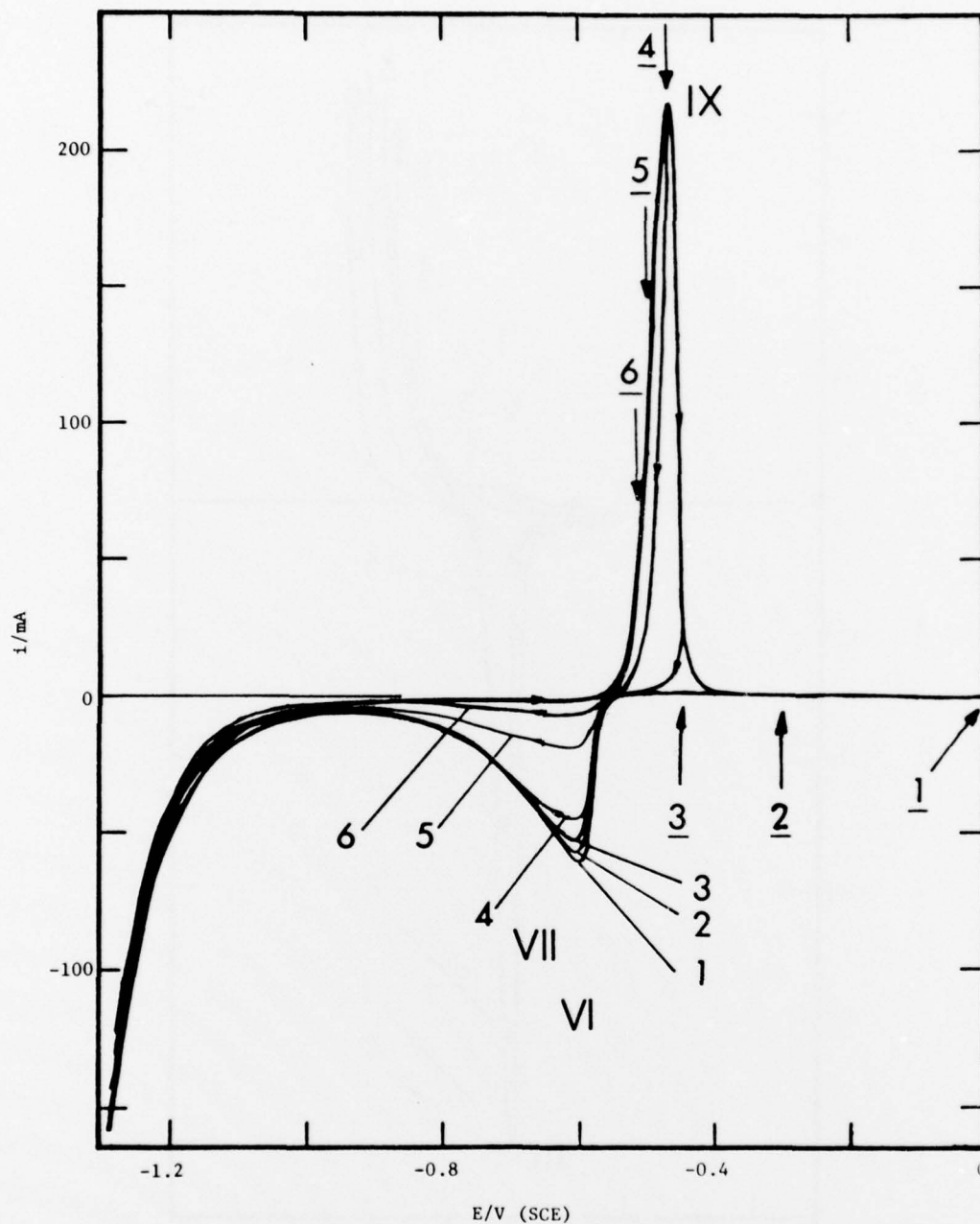


Fig. 18. Cyclic voltammograms on antimonial lead, between hydrogen evolution and 0.0 to -0.5V, at 25°C and 13.9 mV/s, showing effect of decreasing prp on peaks VI + VII.

## DISCUSSION

### IDENTIFICATION OF ELECTROCHEMICAL REACTIONS

The voltammetry indicates that several redox systems are involved. To some extent they can be identified. Thus, peaks III and II clearly represent the reduction and formation of tetravalent lead, and peaks VI + VII and IX the reduction and formation of divalent lead. Each is the major system in its region. The results of Panesar (1971) and Carr et al (1971) on the cyclic voltammetry of  $\alpha$ - and  $\beta$ -PbO<sub>2</sub> surfaces indicate that peaks III and II represent the  $\beta$ -PbO<sub>2</sub>/PbSO<sub>4</sub> system. Peaks VI + VII and IX probably represent the PbSO<sub>4</sub>/Pb system, although the presence of two cathodic activities suggests that it is not so simple. Carr et al (1971) attribute this composite activity to the reduction of a duplex structure comprising PbSO<sub>4</sub> and underlying  $\beta$ -PbO<sub>2</sub>. However, VI + VII is a strong peak even when the positive sweep is reversed well below the potential at which PbO<sub>2</sub> could form (Figure 8).

Other assignments are much less certain. Peak I may represent  $\alpha$ -PbO<sub>2</sub> formation (Panesar, 1971), and peak IV its reduction (Sharpe, 1975). However, Panesar (1971) and Carr et al (1971), finding a relationship between  $\alpha$ -PbO<sub>2</sub> and peak V, consider that the reduction of  $\alpha$ -PbO<sub>2</sub> is represented by peak V, and that the reduction is directly to metallic lead (Carr et al, 1971). Alternatively, peak V may be the reduction of a basic divalent lead compound formed by earlier reduction of  $\alpha$ -PbO<sub>2</sub>. Or, it may be reduction of basic divalent lead formed beneath PbSO<sub>4</sub> in the region positive to  $\sim 0.2V$ , the lower part giving rise to  $V_b$ , the upper to  $V_a$ . The latter appears to be at least a partial explanation for peak V. The fact that it has not been seen negative to peak IX (at 25°) would seem to rule out PbSO<sub>4</sub> as the compound undergoing reduction. Peak VIII may be the reduction of basic divalent lead forming below  $\sim 0.2V$ .

Valeriotte and Gallop (1975) observed two anodic peaks at  $\sim 1.5V$ , at  $-10^\circ C$  and  $-20^\circ C$ , separated by 0.13 and 0.07V, respectively. On the basis of Figure 12(c), which shows the separation between peaks I and II to be  $\sim 0.4V$ , a doublet at the position of peak I is indicated. [Under certain conditions, not determined, a doublet has also been seen in the present work, both at peak I and at peak II, at 25°C.] These peaks were interpreted as a two-stage oxidation of divalent lead. The first stage occurs in the less acidic environment of the film interior and the second at the interface with the electrolyte. The first stage was described in terms of PbSO<sub>4</sub> oxidation in an alkaline environment. However, further analysis and comparison with

potential-step experimental results (Valeriotte and Gallop, 1976) suggests that basic sulphates and/or PbO are oxidized during this stage. At both higher and lower temperatures only one peak was observed.

The interesting anodic peak occurring in the negative sweep at  $-0.5V$  (Figure 3) may be related to an anodic excursion between  $V_a$  and  $V_b$  that one of us (E.M.L.V.) has observed on a rotating electrode, and sometimes on a stationary electrode that was rotating during the early part of the positive sweep, at  $15^\circ C$  and a prp of  $\leq 0.6V$ . The latter is believed to represent reoxidation of metallic lead formed by reduction of basic divalent lead at peak  $V_b$ , the volume contraction due to reduction creating pores and exposing such lead to the electrolyte.

#### EFFECT OF SWEEP VARIABLES

In the positive sweep commencing at hydrogen evolution an anodic peak representing  $PbO_2$  formation is invariably absent (Figures 1, 11, 12, 13, 14). At the same time there is anodic activity in the returning negative sweep where  $PbO_2$  might have been expected to form. However, as reported by Panesar (1971) and here confirmed, such a peak can be seen when cycling at a higher nrp, in his case  $1.2V$ , and the negative sweep is now free of anodic activity. These results indicate that the overpotential for  $PbO_2$  formation is high in the absence of residual  $PbO_2$  from a previous positive sweep, as Simon and Caulder (1975) have suggested. Evidently  $PbO_2$  then forms concurrently with the formation of oxygen, or immediately ahead of it (Carr and Hampson, 1972), and in the returning negative sweep the formation of  $PbO_2$ , thus facilitated, continues and gives rise to anodic activity, or a mixture of anodic and cathodic activity, depending on the particular circumstances. The larger part of the anodic activity is attributed to the reaction of peak I, and each structure shown in Figure 1 and 2 can be seen as a combination of this anodic peak and peak III. Peak IV is possibly responsible for the small valley on its negative side (Figure 3). The anodic activity negative to this may be due to corrosion, the large volume change in reduction setting up mechanical stresses in the film and causing the substrate to be exposed. Sharpe (1975) attributes the whole of the anodic activity to the substrate corrosion.

The overpotential for  $PbO_2$  formation in the  $PbO_2$ -free film increases with decrease in temperature (Figure 12). Relative to a film containing residual  $PbO_2$  it increases from  $\sim 0.7V$  at  $25^\circ C$  to  $\sim 1.9V$  at  $-40^\circ C$ . The increasing anodic current that follows reversal of the positive sweep at  $-40^\circ C$  evidently represents oxygen formation on a surface of increasing  $PbO_2$  content, which indicates that the formation of  $PbO_2$  also facilitates the formation of oxygen.

Two forms of hysteresis are observed: on reversing the sweep the returning current may be higher or lower. A higher current indicates that the process involved has been facilitated or catalysed and the rate is higher despite the less favourable potential. It has been observed only on the

leading side of a peak, as in the onset of oxygen evolution and  $PbO_2$  formation in a  $PbO_2$ -free film (Figures 1, 2, 3, 12), and on peak  $V_b$  (Figure 15). When the current is lower it may be simply because the driving force is lower; it may be even lower if the process has advanced to the point of becoming self-inhibiting. This occurs on the trailing side of the peak in all cases. It also occurs on the leading side of peak III (Figure 6), indicating that a catalytic effect is not involved in  $PbO_2$  reduction. When the current is the same the process is nearly reversible, and this occurs on the leading side of peaks II (Figure 7, 17), IX (Figure 18), and VI (Figure 10). The behaviour on peak IX appears to be consistent with the mechanism for anodic formation of  $PbSO_4$  proposed by Archdale and Harrison (1972) and Weininger (1974): a fast dissolution process on the leading side, followed by precipitation of  $PbSO_4$ , and followed at still higher potentials by a solid state nucleation and growth process for  $PbSO_4$  formation. The latter would occur on the trailing side of peak IX. A fast dissolution process may also be operating on the leading side of peaks VI and II.

A characteristic of the peak shifting that occurs with systematic change of reversal potential is that the direction of shift is opposite to the direction of potential change (Figures 6, 10, 11, 13, 17, 18). It indicates that the overpotential of the process decreases as the extent of reversal decreases. The effect is very small for peaks VI and IX, consistent with a reversible process on their leading side, and relatively large for peaks II and  $V_b$ , consistent with the operation of a catalytic effect in the formation of  $PbO_2$  and the product of  $V_b$ . The shift of the opposite sense shown in Figure 11, in which the potential for oxygen evolution increases 0.2V as the nrp approaches peak IX, suggests that a more perfect film of  $PbSO_4$  is forming and causing the overpotential for  $PbO_2$  formation to increase.

#### ANTIMONIAL LEAD

This work has shown that at  $\sim 0.1V$  there are three anodic peaks and at  $\sim -0.3V$  two cathodic peaks assignable to antimony, rather than the one of each reported by Panesar (1971) and Brennan et al (1974). However, nothing further can be said as to the nature of the reactions; presumably they represent the oxidation of antimony of tri- and pentavalent compounds, and their reduction. The fact that the size of these peaks decreases during the first few cycles indicates a net loss of antimony from the film, until a steady state is reached between its diffusion into the bulk electrolyte and further substrate corrosion. The effect of antimony in lowering the hydrogen overpotential is, of course, well known, and it remains a large effect even to  $-40^\circ$ .

It should be remembered that under certain conditions lead oxidation peaks can also be seen at 0.1V. Therefore, it is possible that in the presence of antimony these oxidations are catalysed and the activity at  $\sim 0.1V$  represents the oxidation of both antimony and lead.

CONCLUSION

This work has provided further information on the cyclic voltammetry of lead and antimonial lead in aqueous sulphuric acid, revealing both more peaks and more information on their response to changes in sweep variables. Cyclic sweeping within narrow regions, which gives rise to additional peak shifting and hysteresis effects, has given further insight into the nature of the reactions. The conditions under which  $PbO_2$  formation can be seen in the positive sweep have been determined and a catalytic effect has been shown to operate in this process. The voltammetry has been extended to  $-40^\circ C$ .

Several findings are of significance to the problem of poor charge acceptance at low temperatures. The adverse effect of antimony on hydrogen overpotential continues to  $-40^\circ C$  but is of greater importance due to the reduced separation between  $PbSO_4$  reduction (peak VII) and hydrogen evolution. Between  $25^\circ C$  and  $-40^\circ C$  there is a reduction of  $\sim 0.07V$  in the separation between  $PbO_2$  formation and oxygen evolution, and the rate of  $PbO_2$  formation is reduced by a factor of  $\sim 500$ . The high rate factor (equivalent to an activation energy of  $\sim 13$  kcal) together with the high overpotential for  $PbO_2$  formation on a  $PbO_2$ -free surface suggests that the charging process is activation controlled. If so, it may be possible to promote it in some way, just as  $PbO_2$  itself seems to do.

ACKNOWLEDGEMENTS

This work was done for Defence Research Establishment Ottawa (DREO) at Cominco's Product Research Centre and at DREO. It is part of an investigation of the charge-acceptance characteristics of the positive electrode of the lead-acid battery at  $-40^\circ$ . The technical assistance of Lloyd D. Gallop of DREO is acknowledged.

REFERENCES

1. G. Archdale and J.A. Harrison, *J. Electroanal. Chem.* 39, 357 (1972).
2. M.P.J. Brennan, B.N. Stirrup and N.A. Hampson, *J. App. Electrochem.* 4, 49 (1974).
3. J.P. Carr and N.A. Hampson, *Chem. Rev.* 72, 701 (1972).
4. J.P. Carr, N.A. Hampson and R. Taylor, *J. Electroanal. Chem.* 33, 109 (1971).
5. D.O. Feder, "Power Sources 3" (D.H. Collins, ed.), p. 88, Oriel Press Newcastle-upon-Tyne (1971).
6. H.S. Panesar, "Power Sources 3" (D.H. Collins, ed.), p. 79, Oriel Press Newcastle-upon-Tyne (1971).
7. T.F. Sharpe, *J. Electrochem. Soc.* 122, 845 (1975).
8. A.C. Simon and S.M. Caulder, "Power Sources 5" (D.H. Collins, ed.), p. 109, Academic Press, London and New York (1975).
9. E.M.L. Valeriotte and L.D. Gallop, "Power Sources 5" (D.H. Collins, ed.), p. 55, Academic Press, London and New York (1975).
10. E.M.L. Valeriotte and L.D. Gallop, "The Kinetics of the Potentiostatic Oxidation of Lead Sulphate Films on Lead in Sulphuric Acid Solution", *J. Electrochem. Soc.*, in press, March (1977).
11. J.L. Weininger, *J. Electrochem. Soc.* 121, 1454 (1974).
12. E. Willihnganz, "Power Sources 5" (D.H. Collins, ed.), p. 43, Academic Press, London and New York (1975).

UNCLASSIFIED

Security Classification

DOCUMENT CONTROL DATA - R & D		
(Security classification of title, body of abstract and indexing annotation must be entered when the overall document is classified)		
1. ORIGINATING ACTIVITY <b>Defence Research Establishment Ottawa National Defence Headquarters Ottawa, Ontario, Canada K1A 0Z4</b>	2a. DOCUMENT SECURITY CLASSIFICATION <b>UNCLASSIFIED</b>	
	2b. GROUP <b>N/A</b>	
3. DOCUMENT TITLE <b>THE CYCLIC VOLTAMMETRY OF LEAD AND LEAD/ANTIMONY BATTERY GRID ALLOY IN AQUEOUS SULPHURIC ACID AT 25°C and -50°C (U)</b>		
4. DESCRIPTIVE NOTES (Type of report and inclusive dates)		
5. AUTHOR(S) (Last name, first name, middle initial) <b>CHANG, Godfrey T. and WRIGHT, Maurice M. of COMINCO, and VALERIOTE, Eugene M.</b>		
6. DOCUMENT DATE <b>JANUARY 1977</b>	7a. TOTAL NO. OF PAGES <b>29</b>	7b. NO. OF REFS <b>12</b>
8a. PROJECT OR GRANT NO. <b>5480-08</b>	9a. ORIGINATOR'S DOCUMENT NUMBER(S) <b>DREO REPORT NO. 753</b>	
8b. CONTRACT NO. <b>2SR5-0020</b>	9b. OTHER DOCUMENT NO.(S) (Any other numbers that may be assigned this document)	
10. DISTRIBUTION STATEMENT <b>UNLIMITED DISTRIBUTION</b>		
11. SUPPLEMENTARY NOTES	12. SPONSORING ACTIVITY <b>DREO</b>	
13. ABSTRACT <p>The cyclic voltammetry of lead and antimonial lead has been studied in 1.25 S.G. H<sub>2</sub>SO<sub>4</sub>, at 25° to -40°, at sweep rates of 0.42 to 42 mV/s, between hydrogen and oxygen evolution and over narrower regions of potential. The latter, coupled with systematic variation of the positive or negative reversal potential, has revealed peak shifting and hysteresis effects which give further insight into the nature of the reactions of the lead/acid battery. The significance of the results to the improvement of charge acceptance at low temperatures is discussed.</p> <p style="text-align: center;">UNCLASSIFIED</p>		

UNCLASSIFIED

Security Classification

KEY WORDS

LEAD/ACID BATTERIES

SULFURIC ACID

LEAD ALLOYS

ANTIMONY

ELECTRICAL MEASUREMENT

LOW TEMPERATURE TESTS

TEMPERATURE COEFFICIENT

CYCLIC VOLTAMMETRY

INSTRUCTIONS

1. **ORIGINATING ACTIVITY:** Enter the name and address of the organization issuing the document.
- 2a. **DOCUMENT SECURITY CLASSIFICATION:** Enter the overall security classification of the document including special warning terms whenever applicable.
- 2b. **GROUP:** Enter security reclassification group number. The three groups are defined in Appendix 'M' of the DRB Security Regulations.
3. **DOCUMENT TITLE:** Enter the complete document title in all capital letters. Titles in all cases should be unclassified. If a sufficiently descriptive title cannot be selected without classification, show title classification with the usual one-capital-letter abbreviation in parentheses immediately following the title.
4. **DESCRIPTIVE NOTES:** Enter the category of document, e.g. technical report, technical note or technical letter. If appropriate, enter the type of document, e.g. interim, progress, summary, annual or final. Give the inclusive dates when a specific reporting period is covered.
5. **AUTHOR(S):** Enter the name(s) of author(s) as shown on or in the document. Enter last name, first name, middle initial. If military, show rank. The name of the principal author is an absolute minimum requirement.
6. **DOCUMENT DATE:** Enter the date (month, year) of Establishment approval for publication of the document.
- 7a. **TOTAL NUMBER OF PAGES:** The total page count should follow normal pagination procedures, i.e., enter the number of pages containing information.
- 7b. **NUMBER OF REFERENCES:** Enter the total number of references cited in the document.
- 8a. **PROJECT OR GRANT NUMBER:** If appropriate, enter the applicable research and development project or grant number under which the document was written.
- 8b. **CONTRACT NUMBER:** If appropriate, enter the applicable number under which the document was written.
- 9a. **ORIGINATOR'S DOCUMENT NUMBER(S):** Enter the official document number by which the document will be identified and controlled by the originating activity. This number must be unique to this document.
- 9b. **OTHER DOCUMENT NUMBER(S):** If the document has been assigned any other document numbers (either by the originator or by the sponsor), also enter this number(s).
10. **DISTRIBUTION STATEMENT:** Enter any limitations on further dissemination of the document, other than those imposed by security classification, using standard statements such as:
  - (1) "Qualified requesters may obtain copies of this document from their defence documentation center."
  - (2) "Announcement and dissemination of this document is not authorized without prior approval from originating activity."
11. **SUPPLEMENTARY NOTES:** Use for additional explanatory notes.
12. **SPONSORING ACTIVITY:** Enter the name of the departmental project office or laboratory sponsoring the research and development. Include address.
13. **ABSTRACT:** Enter an abstract giving a brief and factual summary of the document, even though it may also appear elsewhere in the body of the document itself. It is highly desirable that the abstract of classified documents be unclassified. Each paragraph of the abstract shall end with an indication of the security classification of the information in the paragraph (unless the document itself is unclassified) represented as (TS), (S), (C), (R), or (U).

The length of the abstract should be limited to 20 single-spaced standard typewritten lines, 7 1/2 inches long.
14. **KEY WORDS:** Key words are technically meaningful terms or short phrases that characterize a document and could be helpful in cataloging the document. Key words should be selected so that no security classification is required. Identifiers, such as equipment model designation, trade name, military project code name, geographic location, may be used as key words but will be followed by an indication of technical context.